Document downloaded from:

http://hdl.handle.net/10251/145413

This paper must be cited as:

Gil, A.; Tiseira, A.; García-Cuevas González, LM.; Rodriguez-Usaquen, YT.; Mijotte, G. (09-2). Fast 3-D heat transfer model for computing internal temperatures in the bearing housing of automotive turbochargers. International Journal of Engine Research. https://doi.org/10.1177/1468087418804949


The final publication is available at

https://doi.org/10.1177/1468087418804949

Copyright SAGE Publications

Additional Information

Standard article

# Fast 3-D heat transfer model for computing internal temperatures in the bearing housing of automotive turbochargers

A. Gil, L.M. García-Cuevas, A. Tiseira, T. Rodríguez Usaquén

CMT-Motores Térmicos, Universitat Politècnica de València, Spain

## Abstract

Each of the elements that make up the turbocharger has been gradually improved. In order to ensure that the system does not experience any mechanical failures or loss of efficiency, it is important to study which engine operating conditions could produce the highest failing rate. Common failing conditions in turbochargers are mostly achieve due to oil contamination and high temperatures in the bearing system. Thermal management becomes increasingly important for the required engine performance. Therefore, it has become necessary to have accurate temperature and heat transfer models.

Most thermal design and analysis codes need data for validation; often the data available falls outside the range of conditions the engine experiences in reality leading to the need to interpolate and extrapolate disproportionately. This paper presents a fast 3D heat transfer model for computing internal temperatures in the central housing for non-water cooled turbochargers and its direct validation with experimental data at different engine operating conditions of speed and load.

The presented model allows a detailed study of the temperature rise of the central housing, lubrication channels, and maximum level of temperature at different points of the bearing system of an automotive turbocharger. It will let to evaluate thermal damage done to the system itself and influences on the working fluid temperatures, which leads oil coke formation that can affect the performance of the engine. Thermal heat transfer properties obtained from this model can be used for to feed and improve a radial lumped model of heat transfer that predicts only local internal temperatures[1]. Model validation is illustrated and finally the main results are discussed.

## Keywords

Turbocharger, thermal characterization, 3D heat transfer model, FEM, central housing, bearing system, oil damage.

**Corresponding author:**
Andres Omar Tiseira, CMT – Motores Térmicos Universitat Politècnica de València, Camino de Vera, s/n, 46022 Valencia, Spain.
Email: anti1@mot.upv.es

# Introduction

The need for improved fuel economy and reduced emissions has led to great achievements in engine performance and control. As more effort is put into obtaining higher efficiencies and lower emissions [2], the role of the turbocharger becomes more and more important, increasing the complexity of the system.The turbocharger system has been used for a long time in the boost of automotive engines [3]. The system is an important piece for the new generation of engines that must comply with Euro 6 standard or in US the Tier 3 Vehicle Emissions and Fuel Standard Program [4].
Each of the elements that make up the turbocharger has been gradually improved. In order to ensure that the system does not experience any mechanical failures or loss of efficiency, it is important to study which engine operating conditions could produce the highest failing rate. Common failing conditions in turbochargers are mostly achieve due to oil contamination [5]. which results in damaged blade caused by contamination from dirt or other particles entering the turbine or compressor housing, low power or boost caused by a gas leak or blocked cooler restricting air injection, excessive exhaust gas temperatures, worn or excessive clearance caused by low oil. Thermal management of the engine becomes increasingly important for the required engine performance[6] .Therefore it has become increasingly important to have accurate temperature and heat transfer models as well as data to validate them.

Szymko et al. [7] contribute to this area by providing extensive experimental data in a large range of conditions of the turbine performance under pulsating flow. Serrano et al. [8] study the robustness of several turbochargers ingestion of different elements such as screws, sand or water with the compressor. Galindo et al. [9] also study the mechanical behaviour of turbochargers with intermittent stops of the lubricating oil flow.
In the literature, several studies about turbocharger endurance and loss of efficiency have been found. Studies based on the behaviour of the different parts of the turbocharger affecting its final performance is studied in detail, such as mechanical efficiency [10], computation of power friction losses due to journal bearing [11], even examination of mechanical preload and bearing clearance to improve the rotor dynamic performance and reduce the friction losses [12].

Most thermal design and analysis codes need data for validation; often the data available falls outside the range of conditions the engine experiences in reality leading to the need to interpolate and extrapolate excessively. Some works focus their study on aerodynamic or acoustic phenomena, looking for flow disturbance sources in either the compressor or the turbine side. Drewczynski et al [13] uses methods of load transfer affect rotor blade stress and displacement levels during one period of rotation. Filsinger et al [14] study the vibration behaviour of an axial turbocharger turbine by using an approach to unidirectional coupled Computational Fluid Dynamic-Finite Element Method (CFD-FEM) Analysis. Other 3D modelling studies of heat transfer in turbochargers has been carried out by changing the materials of the turbine blade and assuming car is running at higher speeds [15].

Different simple models have been developed during the last years that improve the prediction of the turbocharger heat transfer phenomena. Although these models produce good results when computing the turbine outlet temperature, those models focus on the axial heat transfer paths [16]–[18] and lack the capability of producing detailed results about the internal thermal state of the turbocharger, so the oil degradation phenomena are not predicted easily.
In this work, a fast 3D heat transfer model for computing internal temperatures in a bearing housing for non-water cooling turbochargers is presented. In addition, experimental tests of

thermal behaviour in the bearing system at different engine operating points of speed and load are presented and used for the model validation.

The paper is divided in two main parts the first deals with the description of the experimental thermal characterization carried out in the turbocharger, providing data of temperatures in the bearing housing and close to the narrow channels of the lubrication system. In a second stage, the 3D heat transfer model, global setup and validation is presented. This second part describes the thermal coefficients determination that serve as base for modelling other turbochargers. The advantage of computing the internal temperature in the central housing, lubrication channels, and maximum level of temperature at different points in the bearing system makes the reduction of experimental tasks. Besides, this model will let to evaluate thermal damage done to the system itself, as well as influences on the working fluid temperatures which leads oil coke formation, that can affect the performance of the engine [19]. The thermal heat transfer properties such as conductivity and capacitances obtained from this model has been used for to feed and improve a radial lumped model of heat transfer [1] that predicts temperatures only at local points in the turbocharger central housing. The validation applied for a not water cooled turbocharger is illustrated and finally the main results are discussed.

# Methodology

The use of this methodology pretends to evaluate the temperature under steady conditions for the turbocharger bearing housing under different engine operating points of regime and load. The turbocharger thermal characterization is performed in an engine test bench. Characterization results are considered valid if the temperatures of oil, turbine side and compressor side, bearings and housing have been stabilized during the experiments.

The model is developed in several steps and feed with boundary conditions from the experimental data. In order to generalize the process for any engine operating condition in non-water cooled turbocharger geometries, these boundary conditions seek to be easy to measure in engine test benches or known by turbocharger manufacturers.

The figure 1 shows the method steps followed to study the heat transfer inside the bearing housing. This model can be used as a diagnostic tool to evaluate oil coking, one of the most common failing conditions in turbochargers.

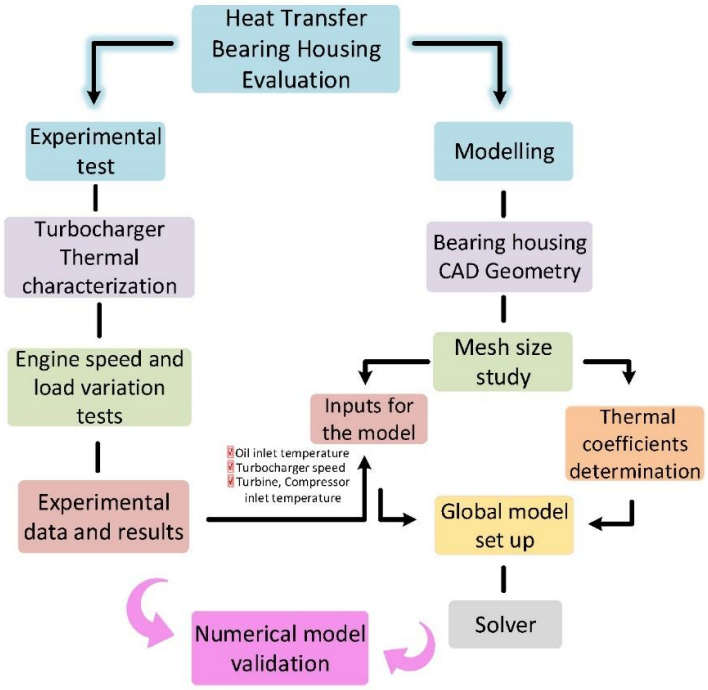


**Figure 1.** Heat transfer methodology to evaluate internal temperatures in the turbocharger bearing housing.

## Turbocharger Experimental Tests

An experimental test bench for stationary engines has been used for model calibration. The system layout has as main elements a Diesel engine (E), a non-water cooled turbocharger (T), and an independent lubrication system (L) that feeds the turbocharging system. Figure 2 shows the sketch of the engine test bench used for the turbocharger thermal characterization.

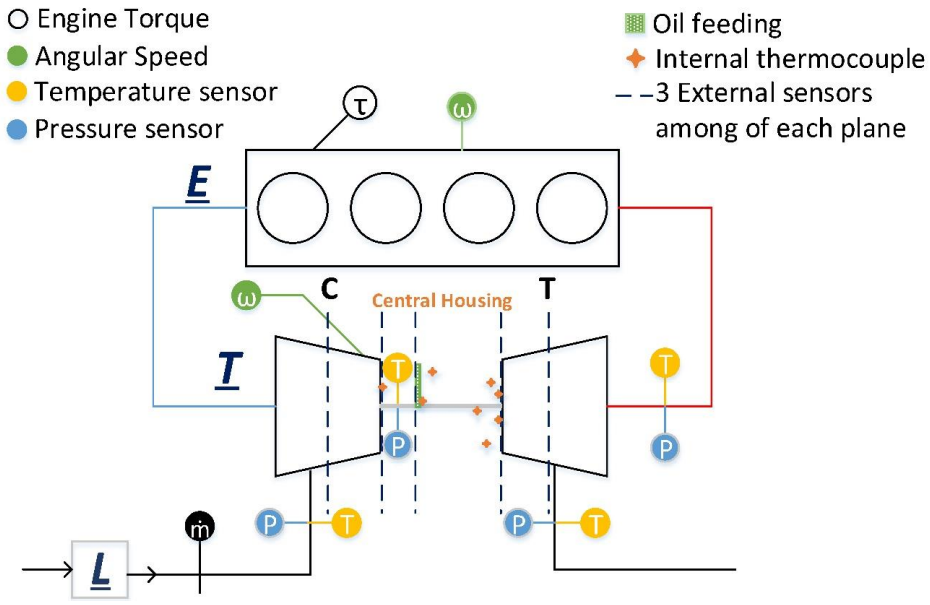


**Figure 2.** Schematic layout of experimental set-up for thermal characterization in turbochargers.

Engine-operating points at different speed and load conditions have been tested. Experimental information was available for the mass flows of gases and fluids, the turbocharger speed, the temperature in the external sections of the turbocharger as well as the internal temperature in points of the turbocharger bearing housing.

The table 1 contains the specifications of the transducers used in the experiments, including their expanded uncertainty. All Turbocharger temperature sensors and oil outlet circuit were thermally insulated.

**Table 1.** Specifications of the transducers used in the experiments.

| Variable Measured | Type | Range | Uncertainty |
|---|---|---|---|
| Temperatures | K-Type thermocouples | 273 (K) to1100(K) | ±2.2 (K) |
| Internal Temperatures | K-Type thermocouples | 273 (K) to 1100 (K) | ±2.2 (K) |
| Oil mass flow | Coriolis flow meter | 0 to 100 (kg/h) | 1 (kg/h) |
| Compressor and turbine mass flow | Thermal flow meter | 0 to 600 (kg/h) | ±2% |
| Pressure | Piezo resistive | 0 to 500 (KPa) | 0.05% full scale |
| Turbocharger speed | Inductive | 0 to 400 (kr/min) | 500 (r/min) |

For each test, the parameters of engine speed, torque, turbine gas inlet temperature, as well as oil inlet temperature for the turbocharger have been controlled and held constant.

Experimental evolution of temperatures under steady conditions are shown in figure 4 for two segments of the turbocharger bearing housing strongly influential in the oil coke formation in the turbocharger bearing system. One of them located close to the radial bearing on the turbine side and another at the bearing housing (drain wall).

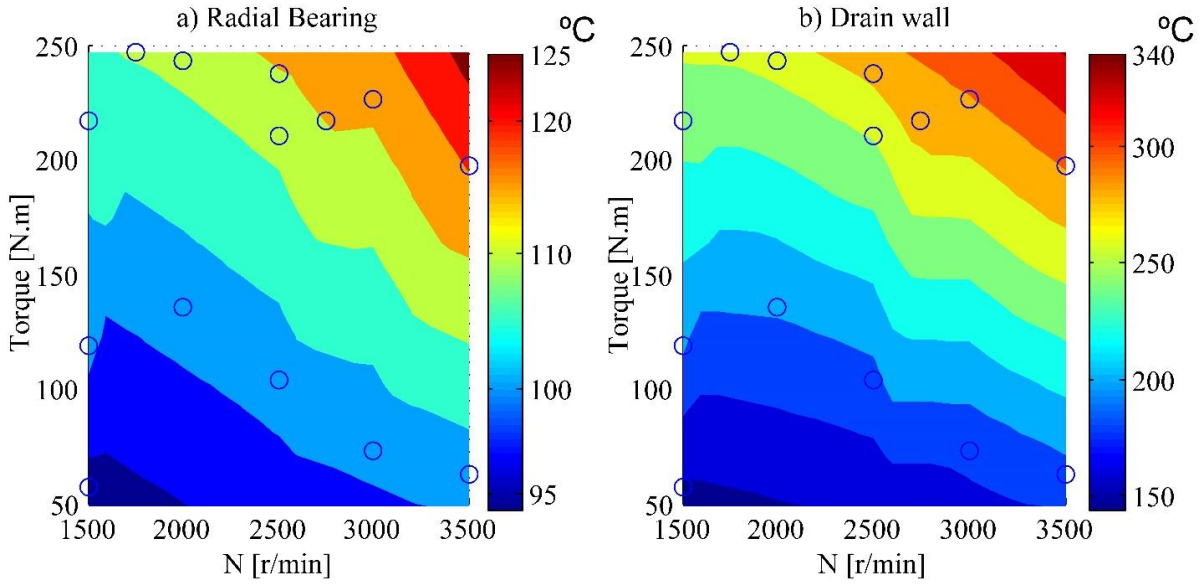


**Figure 3.** Internal temperatures in turbocharger central housing steady state.

## FEM Bearing housing model

The CAD model is done considering a geometric simplification in order to make the model fast calculation. It consists of the lubrication system, the bearings and shaft. The turbocharger compressor and turbine housings are excluded in order to simplify the complex 3D geometry; however, the related boundary conditions are imposed to get the appropriate trade off. The figure 4 shows the bearing housing and the detailed bearing system for this study.

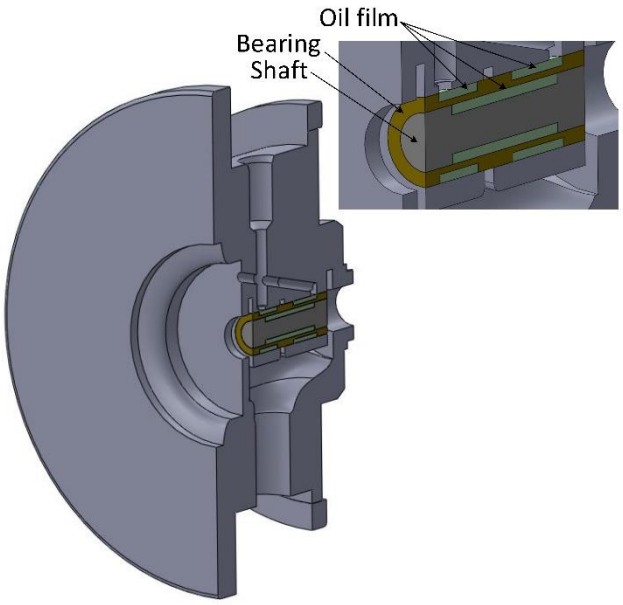


**Figure 4.** Turbocharger 3D bearing housing geometry.

## Mesh Independence Study

The central housing uses a discrete element method model of the wire mesh. Discrete element methods are relatively computationally intensive, which limits the length of either a simulation or the number of particles. A numerical investigation of mesh sensitivity is done. The setup of the geometry and refinement of mesh have been studied to obtain a good extraction of results in a short calculation time

The element sizes studied were 0.002, 0.001, 0.0008 and 0.0005 m for the global mesh grid of the bearing housing in one engine operating point of high speed and load. Figure 5, shows the time of calculation Vs the root mean square error (RMSE) between the experimental and simulations for the four mesh sizes used.

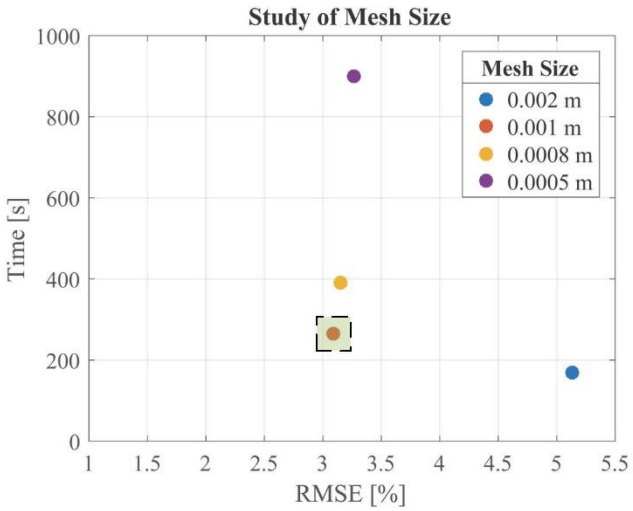


**Figure 5.** Calculation time vs root mean square error (RMSE) using four mesh sizes.

The selection of the best element is systematically chosen to a size of 0,001 m. A refinement of mesh produces an increase in the computation time; besides, the relative difference error with the experiments is not very significant.
In order to reduce the time of calculation without affecting the conclusions the compressor side the mesh size was set to 0.005m. It is because the low temperature of the air that the compressor is ingesting at the inlet plus the fact that most of the temperature rise occurs in the diffuser, where velocity is exchanged for pressure typically keeps the operating temperature of the compressor wheel well below the compressor discharge temperature.

## Inputs for the FEM model

The purpose is to impose the boundary conditions as inputs easy to measure in engine test bench or known by the manufacturers of turbocharger in order to generalize the process for any engine operating condition in non-water cooled turbocharger geometries. The figure 6 shows the input conditions of temperature, settled in the central housing thanks to experimental data available.  The backplate turbine has been discretised in two regions since the exhaust manifold of the engine has greater influence in on one side of the backplate turbine.

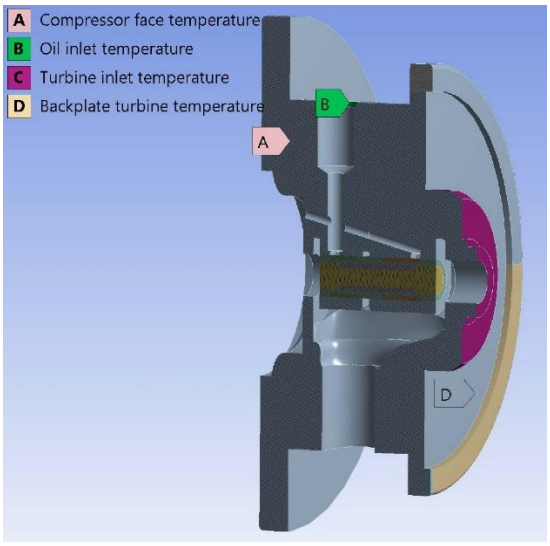


**Figure 6.** Boundary conditions of temperature.

The lubrication system is discretized into three sections. The figure 7 shows the discretization that will be used for heat transfer coefficients determination. The temperature in section 3 is obtained by taking into account the mechanical friction losses ($\dot{W}_{FL}$) and heat flux ($\dot{q}$) to the oil and calculated as a virtual source term of heat flux ($\dot{q}$)'.

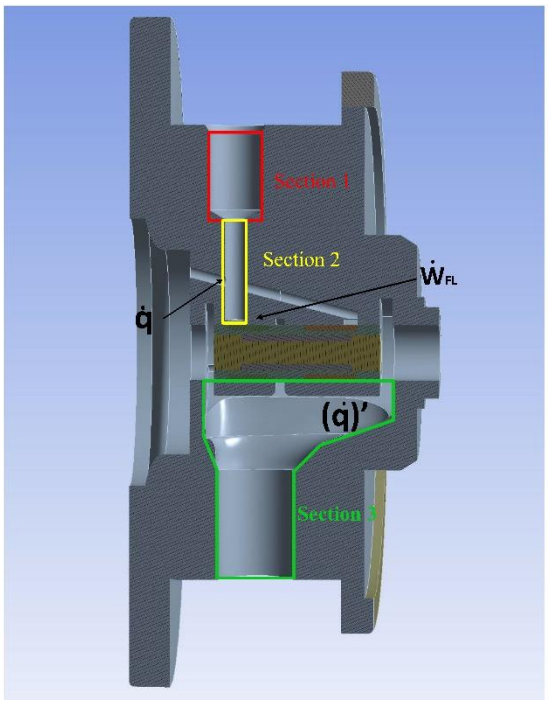


**Figure 7.** Discretization in the bearing housing lubrication system.

From figure 7, a mean temperature in each section of the fluid is imposed as well as the rotating conditions in the shaft and the bearing. The rotational speed of the bearing is adjusted to 50% of the speed of rotation of the shaft [20]. The table 2 shows the total set of boundary conditions for to simulate the internal heat transfer in the turbocharger in steady state conditions.

**Table 2.** Boundary conditions.

| | |
|---|---|
| Temperature | At compressor inlet<br>At oil inlet<br>At turbine Inlet |
| Convective film coefficients in the lubrication system | In section 1<br>In section 2<br>In section 3 |
| Rotation Speed | Of the Bearings<br>Of the shaft |
| Mean temperature in each of the lubricating sections | |

## Thermal coefficients determination

The lubrication system exchanges heat via convection with the bearing housing; thermal convective coefficients have been calculated in each of the discretized sections of the lubrication circuit (See figure 7).
A heat transfer correlation based on Nusselt number [21] for laminar flow is used in the model and shown in equation (1). This equation can be used for steady state conditions in short or long tubes, forced convection and any type of fluid.

$$Nu = 3.66 + \frac{0.065\, Re\, \mathrm{Pr}\frac{D}{L}}{1+0.04\left(Re\, \mathrm{Pr}\frac{D}{L}\right)^{2/3}} \qquad (1)$$

The D and L terms represent the diameter and the length of the tube section that interacts with the fluid. As the length of the tube increases, the number of Nusselt tends to 3.66, being this the result for a wall temperature uniform when the temperature range is fully developed.
The table 3 shows the effective diameter and effective length used in each of the three discretized sections of the lubrication system.

**Table 3.** Geometric data of the ducts.

| | Section 1 x10-3 | Section 2 x10-3 | Section 3 x10-3 |
|---|---|---|---|
| $D_{Eff}$ (m) | 9,05 | 4,18 | 13,48 |
| $L_{Eff}$ (m) | 13,51 | 17,7 | 24,78 |

The Reynolds number can be obtained using equation (2). It involves the mass flow rate, and the ($\mu$) term is the viscosity of the oil.

$$Re = \frac{4 \cdot \dot{m}}{\pi \cdot \mu \cdot D} \quad (2)$$

In the three sections, it was found that the flow is laminar with values between 91.4 and 457 for all engine-operating conditions measured.

Prandtl number is related with temperature variations and it can be obtained through the product of viscosity and specific heat of the oil, divided by thermal conductivity of the material, as shown in equation (3).

$$Pr = \frac{\mu \, C_P}{k} \quad (3)$$

With the use of dimensionless numbers, convective conductance for the three lubrication sections in the BH of the turbocharger can be calculated using equation (4).

$$h = \frac{N_u \cdot \lambda}{D} \quad (4)$$

From equation 4, lambda is the conductivity at the temperature of the fluid. Figure 8 shows the convective heat transfer coefficients obtained for the 5W40 oil under different engine operating conditions.

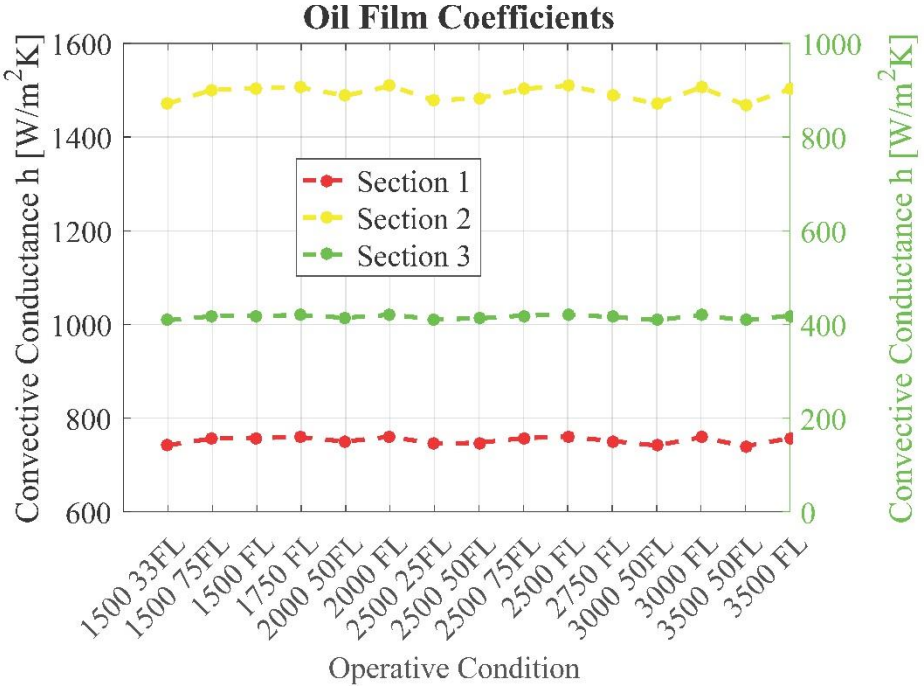


**Figure 8.** Oil convective coefficients for three lubrication sections in the BH of the turbocharger.

## Global model set up

For the global mesh set up, experimental data was used to set compressor backplate and turbine face temperatures of the bearing housing. In the compressor backplate data from three temperature surface probes (distributed every 120 degrees) were used.
Heat gradients in the turbine side has been also consider, since the turbine is the hottest spot of the turbocharger. Experimental data has been used for to obtain a general expression of the central housing turbine side.
The figure 9 a) shows the correlation obtained between the gas inlet temperature and the temperature of central housing turbine side. Additionally, the figure 9 b) is a coefficient of adjustment (C (Op)) that helps to take into account the variations of temperature according the engine operating condition.

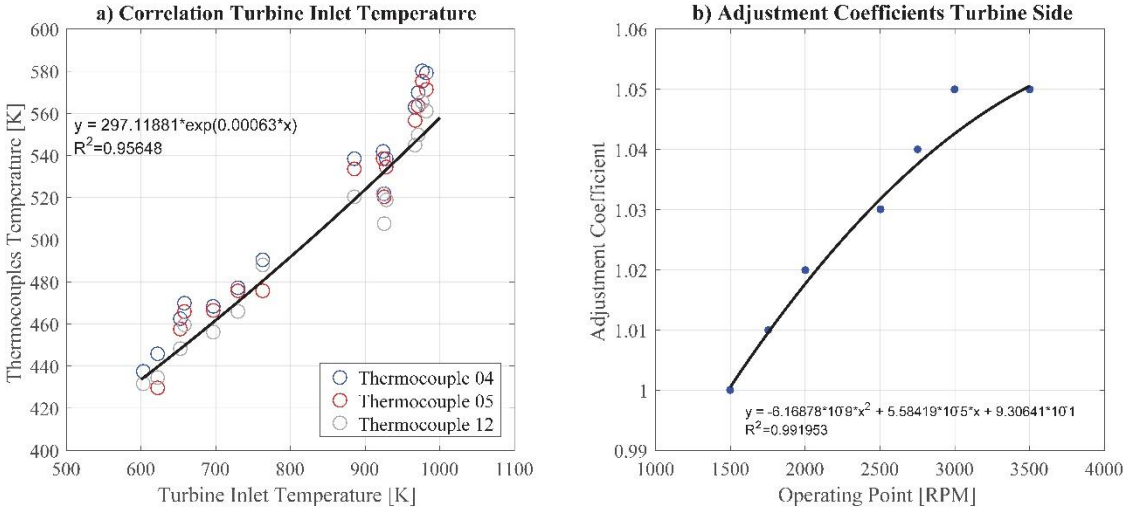


**Figure 9.** Correlations used to determine temperature in the bearing housing (turbine side).

From figure 8, it can be obtained the equation (5) used in the model for to impose the temperature in the turbine wheel side.

$$T_{BH\ Turbine}(T_{iT}, Op) = C(Op) \cdot 297.11881 \cdot e^{0.00063 \cdot T_{eT}} \quad (5)$$

Where:

$$C(Op) = -6.16878 \cdot 10^{-9} \cdot \mathrm{Op}^2 \ + \ 5.58419 \cdot 10^{-05} \cdot \mathrm{Op} \ + \ 9.30641 \cdot 10^{-01} \quad (6)$$

Thermodynamic properties. The thermodynamic material properties of the bearing housing was also set. For the body geometry of the central housing, the material is assumed cast iron. A study of the cast iron thermal conductivity depending on temperature can be found in [22] and the expression used it is represented in the figure 10. Equations 7 and 8 are specific heat and thermal conductivity expressions obtained and used in the bearing housing of the model.

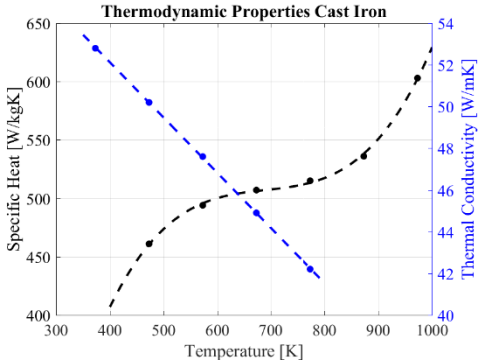


**Figure 10.** Cast iron thermodynamic properties.

$$C_p \text{ (ci)} = 3.5556 \,.\, 10^{-6}.T^3 - 7.3513.10^{-3}\,T^2 + 5.1158 + T - 6.9092.10^2 \quad (7)$$

$$k \text{ (ci)} = -0.0265\,.T + 62.725 \quad (8)$$

The performance and robustness in the bearings are represented in this model using as a material silicon nitride properties. The combination of thermal, dielectric, wear, and superior high-temperature mechanical properties has led to implementation of silicon nitride ball bearing [23] in most turbochargers applications. The figure 11 shows the specific heat and thermal conductivity of the silicon nitride ($Si_3N_4$) [24]. Equations 9 and 10 are expressions of the specific heat and thermal conductivity respectively used in bearings of the model.

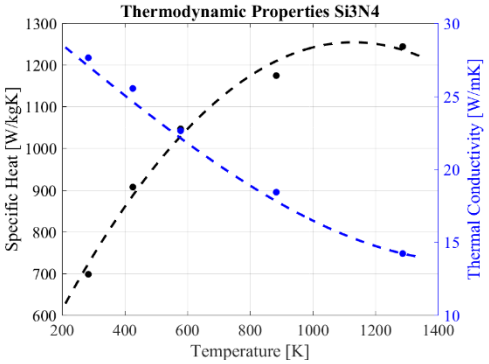


**Figure 11.** Thermodynamic properties silicon nitride.

$$C_p \text{ (Si3N4)} = -7.288564\,.\,10^{-4}.T^2 + 1.658428 + T + 3.109180.10^2 \quad (9)$$

$$k \text{ (Si3N4)} = -3\,.\,10^{-9}.T^3 - 1\,.\,10^{-6}.T^2 - 0.0174.T + 32.045 \quad (10)$$

The gamma titanium aluminide $C_p$ ($\gamma$-TiAl) has been a key drive for turbocharger shaft application [25]–[27] and for reducing turbo lag. Its lightweight reduces rotational inertia and the power boost time. The thermal conductivity and the specific heat based on gamma titanium aluminide used in this heat transfer model is set by using the equation (11) and (12) for ranges between 25 C to 760 C and 400 C to 1430 C respectively [28]

$$k\,(\gamma\text{-TiAl}) = 21.7959 + 8.1633 \cdot 10^{-3} \cdot T \quad (11)$$

$$C_p\ (\gamma\text{-TiAl}) = 0.6324 + 7.44 \cdot 10^{-5} \cdot T - 2{,}07 \cdot 10^{-7} \cdot T^2 + 2.97 \cdot 10^{-10} \cdot T^3 \quad (12)$$

The inputs of fluid physical properties have been also considered on the heat transfer process. The figure 12 shows the thermodynamic properties values for a 5W40 new engine oil. The thermodynamic properties of the oil have been used to determine convective coefficients in the lubrication system.

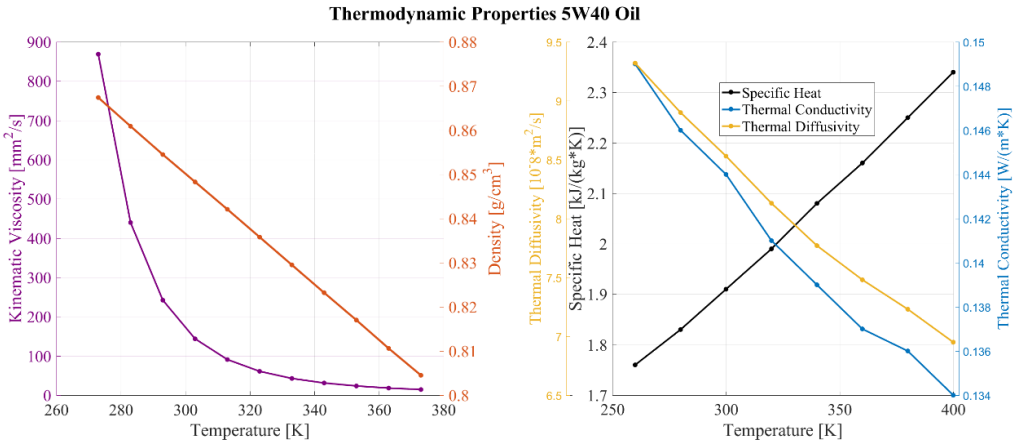


**Figure 12.** Thermodynamic properties 5W40 Oil.

# Model Validation

The numerical solution is made using the FEM. The validation was done using 15 engine-operating points at different speeds and loads. For the validation, the same input parameters obtained in the fitting procedure were used. The experimental temperature of every engine operative condition was set in the boundary conditions (see table 2). The table 4 shows the values of temperature and turbocharger speed imposed for three of the points validated.

Table 4. Boundary condition values for three engine-operating conditions

| Engine Speed (r/min) | Load (%) | Temperature [K] | | | Turbocharger Speed (r/min) | Oil film coefficients [$W/m^2K$] | | |
|---|---|---|---|---|---|---|---|---|
| | | Turbine | Compressor | Oil Inlet | | Section 1 | Section 2 | Section 3 |
| 2500 | 75 | 886.2 | 333.2 | 361.4 | 215000 | 1482.7 | 747.6 | 412.7 |
| 2750 | 100 | 970.8 | 337.4 | 360.9 | 230125 | 1490.8 | 751.2 | 416 |
| 3000 | 50 | 651.8 | 333.2 | 357.3 | 166964 | 1471 | 741.8 | 409.2 |

The figure 13 shows all internal thermocouples location in the central housing where the direct experimental data were taken for model validation.

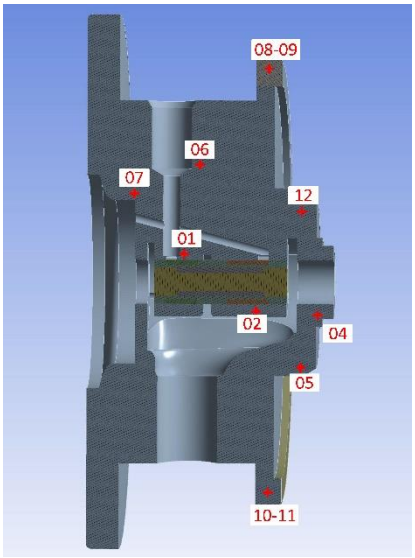


**Figure 13.** Bearing housing temperature points.

Figures 14 to 16 show the validation of this model in each particular point in the central housing and differences of temperature with the experimental measurements in the turbocharger. As regards external temperatures, turbine backplate (nodes 09-11) show the main error. This seems to affect to a lesser degree the errors in the predictions for the other nodes. Although radiation was not considered in this model, it is necessary to study this heat transfer phenomena interactions in the turbocharger, especially in the turbine side where the engine exhaust manifold has some influence with radiation.
Maximum deviation corresponds to the temperature in 11 Point (backplate turbine) at 2750 r/min and full load, with a delta value of 13K. The remainder internal temperatures of the bearing housing of the turbocharger are modelled with less difference deviation and a relative error less than 2%.

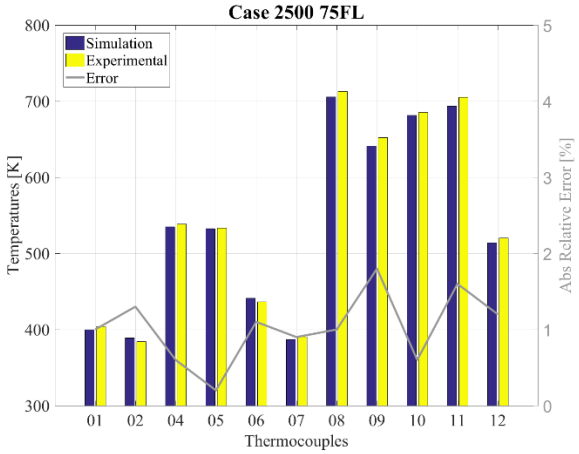


**Figure 14.** Validation of 2500 r/min and 75% of full load.

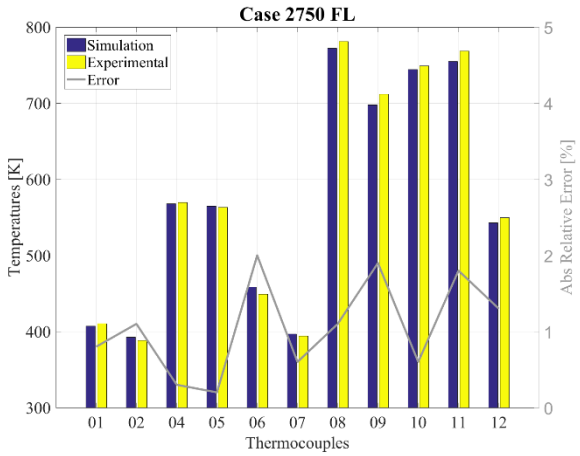


**Figure 15.** Validation of 2750 r/min and full load.

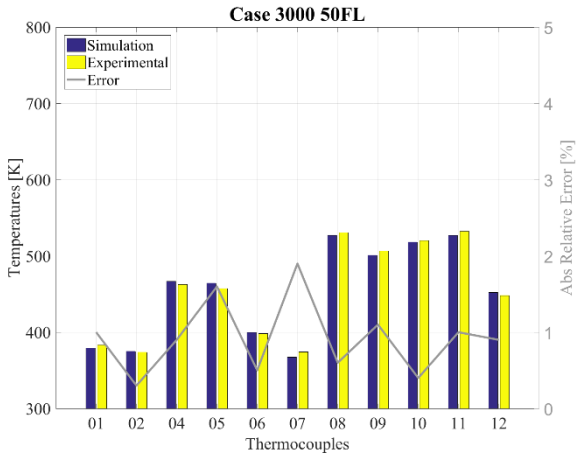


**Figure 16.** Validation of 3000 r/min and 50% full load.

Figure 17 shows the heat gradients along the turbocharger bearing housing for three of the operating points already presented. Under steady state conditions, the difference in temperature in the backplate compressor is small; the heat flux in the central housing at low engine operating conditions becomes predominantly axial Figure 17 (c). This explains the good results obtained in previous 1D axial models, which only exchanged heat with the oil through node H2 [16]. However, variances exist in the turbine side especially at engine operating points of high load and high speed Figure 17 (a) and (b). The heat exchanges are bigger between the external backplate turbine and the internal surface where the turbine wheel is located. The axial heat flow hypothesis is less robust in that zones and the 3D model improve the results when the temperature of the bearings and close to the turbine is required. This is interesting when investigating oil thermal damage such as that produced during engine hot stops conditions. The model is even able to produce results for the temperature distribution along the shaft thanks to detailed solution of heat fluxes performed by means of finite elements.

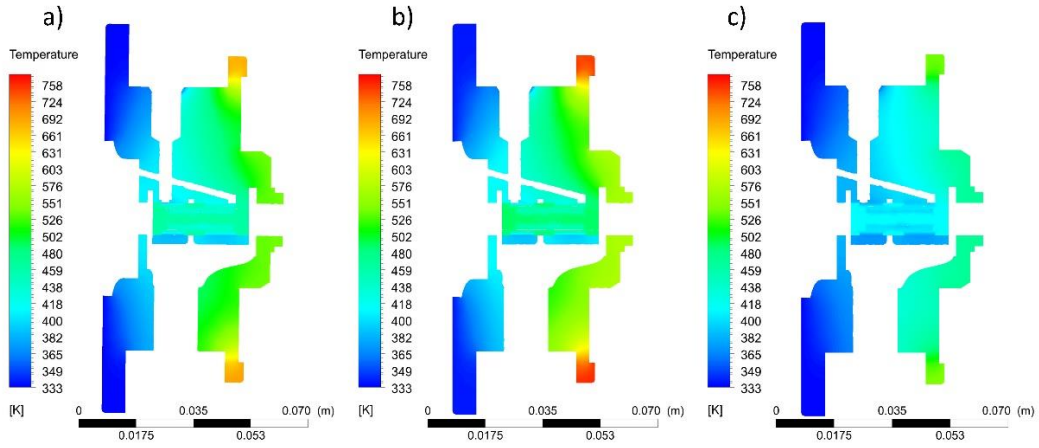


**Figure 17.** Internal temperatures central housing steady state for 2500 75%FL- 2750%FL and 3500 50%FL engine operating conditions.

## Summary/Conclusions

Heat transfer in the turbocharger bearing housing has been studied using FEM numerical solution. The central housing uses a discrete element method model of the wire mesh. The best element to simulate the steady state conditions was systematically chosen to a size of 0,001 m because of the time of calculation spent and the difference error with the experiments. The mesh size settings is the same for all engine-operating points simulated.

To simplify the complex 3D geometry of the turbocharger, the design of the compressor and turbine housings were excluded. However, the related boundary conditions were imposed to get the appropriate trade off.

In the turbine side, a correlation has been obtained as function of the gas inlet temperature. The correlation adopted as input condition shows a good agreement in all operating conditions of speed and load simulated. The relative error is less than 2% for the side where turbine wheel is located (thermocouples 04, 05 and 12).

Maximum delta temperature deviation was 13K for points located in the backplate turbine for an engine operating point of 2750 r/min and full load.

In the compressor side, the heat flux becomes predominantly axial. While the turbine side the heat exchanges are bigger. This model has the capability to produce results for the internal thermal state of the turbocharger, and improve the prediction of previous 1D or radial turbocharger models.

The model is able to compute internal temperatures in the shaft and can be used as a diagnostic tool to evaluate oil-coking phenomena, one of the most common failing conditions in turbochargers.

**Acknowledgments**

Authors want to acknowledge the “Apoyo para la investigación y Desarrollo (PAID)” grant for doctoral studies (FPI-2016-S2-1354).

# Bibliography


[1] J. R. Serrano, A. Tiseira, L. M. García-Cuevas, T. Rodriguez, and G. Mijotte, “Fast 2-D Heat Transfer Model for Computing Internal Temperatures in Automotive Turbochargers,” *SAE World Congr. WCX 17*, no. 2017-01–0513, 2017.

[2] E. Khalife, M. Tabatabaei, A. Demirbas, and M. Aghbashlo, “Impacts of additives on performance and emission characteristics of diesel engines during steady state operation,” *Prog. Energy Combust. Sci.*, vol. 59, pp. 32–78, 2017.

[3] R.-R. H. T. Taylor, Douglas Richard, *Boxkite to Jet: The Remarkable Career of Frank B.Halford (Historical)*. 1999.

[4] F. Payri, P. Olmeda, J. Martín, and R. Carreño, “Experimental analysis of the global energy balance in a DI diesel engine,” *Appl. Therm. Eng.*, vol. 89, pp. 545–557, 2015.

[5] D. Polichronis, R. Evaggelos, G. Alcibiades, G. Elias, and P. Apostolos, “Turbocharger Lubrication - Lubricant Behavior and Factors That Cause Turbocharger Failure,” *Int. J. Automot. Eng. Technol.*, vol. 2, no. 1, pp. 40–54, 2013.

[6] H. Aghaali, “On-Engine Turbocharger Performance Considering Heat Transfer,” 2012.

[7] S. Szymko, R. F. Martinez-Botas, and K. R. Pullen, “Experimental Evaluation of Turbocharger Turbine Performance Under Pulsating Flow Conditions,” in *Volume 6: Turbo Expo 2005, Parts A and B*, 2005, pp. 1447–1457.

[8] J. R. Serrano, B. Tormos, K. L. Gargar, and F. Bouffaud, “Study of the Effects on Turbocharger Performance Generated by the Presence of Foreign Objects at the Compressor Intake,” *Exp. Tech.*, vol. 37, no. 2, pp. 30–40, Mar. 2013.

[9] J. Galindo, J. R. Serrano, V. Dolz, and M. A. López, “Behavior of an IC Engine Turbocharger in Critical Condition of Lubrication,” *SAE Int. J. Engines*, vol. 6, no. 2, pp. 797–805, 2013.

[10] F. Payri, J. R. Serrano, P. Olmeda, A. Paez, and F. Vidal, “Experimental Methodology to Characterize Mechanical Losses in Small Turbochargers,” in *Volume 5: Industrial and Cogeneration; Microturbines and Small Turbomachinery; Oil and Gas Applications; Wind Turbine Technology*, 2010, pp. 413–423.

[11] M. Deligant, P. Podevin, and G. Descombes, “CFD model for turbocharger journal bearing performances,” *Appl. Therm. Eng.*, vol. 31, no. 5, pp. 811–819, 2011.

[12] K. Sim, Y.-B. Lee, and T. H. Kim, “Effects of Mechanical Preload and Bearing Clearance on Rotordynamic Performance of Lobed Gas Foil Bearings for Oil-Free Turbochargers,” *Tribol. Trans.*, vol. 56, no. 2, pp. 224–235, Mar. 2013.

[13] M. Drewczynski and R. Rzadkowski, “A stress analysis of a compressor blade in partially blocked inlet condition,” *Proc. Inst. Mech. Eng. Part G J. Aerosp. Eng.*, vol. 230, no. 5, pp. 934–952, Apr. 2016.

[14] D. Filsinger, J. Szwedowicz, and O. Schäfer, “Approach to Unidirectional Coupled CFD–FEM Analysis of Axial Turbocharger Turbine Blades,” *J. Turbomach.*, vol. 124, no. 1, p. 125, Jan. 2002.

[15] S. M. Shafi, V. V Ramakrishna, and S. Rajasekhar, “Thermal Analysis of Turbocharger by Varying Materials.”

[16] R. D. Burke, P. Olmeda, F. J. Arnau, and M. Reyes-Belmonte, “Modelling of turbocharger heat transfer under stationary and transient engine operating conditions,” in *Institution of Mechanical Engineers - 11th International Conference on Turbochargers and Turbocharging*, 2014, pp. 103–112.

[17] A. Romagnoli and R. Martinez-Botas, “Heat Transfer Analysis in a Turbocharger Turbine:

An Experimental And Computational Evaluation," *Appl. Therm. Eng.*, vol. 38, no. May 2012, pp. 58–77, 2012.
[18] M. Cormerais, P. Chesse, and J.-F. Hetet, "Turbocharger Heat Transfer Modeling Under Steady and Transient Conditions," *Int. J. Thermodyn.*, vol. 12, no. 4, pp. 193–202, 2009.
[19] I. Miyata, S. Hirano, M. Tanada, and K. Fujimoto, "Mechanism of Turbocharger Coking in Gasoline Engines," *SAE Int.*, no. JSAE 20159223, pp. 1–15, 2015.
[20] D. Deng, F. Shi, L. Begin, I. Du, and General Motors, "The Effect of Oil Debris in Turbocharger Journal Bearings on SubSynchronous NVH," *SAE Int.*, vol. 2015-01–12, no. April, 2015.
[21] R. S. Subramanian, "Heat transfer to or from a fluid flowing through a tube."
[22] S. M Shelton, "Thermal conductivity of irons and steels over the temperature tange 100 to 500c," *Part Bur. Stand. J. Res.*, vol. 12, no. 5, pp. 619–620, 1934.
[23] D. Zeppei, S. Koch, and A. Rohi, "Ball Bearing Technology for Passenger Car Turbochargers," *Mot. Zeitschrift - Springer*, vol. 77, no. 11/2016, pp. 26–31, 2016.
[24] J. M. Sci, D. De Faoite, D. J. Browne, F. R. Chang-Díaz, and K. T. Stanton, "A review of the processing, composition, and temperature-dependent mechanical and thermal properties of dielectric technical ceramics."
[25] A. K. Sachdev, K. Kulkarni, Z. Z. Fang, R. Yang, and V. Girshov, "Titanium for automotive applications: Challenges and opportunities in materials and processing," *Jom*, vol. 64, no. 5, pp. 553–565, 2012.
[26] T. Tetsui, "Development of a TiAl turbocharger for passenger vehicles," *Mater. Sci. Eng. A329–*, vol. 331, no. 2016, pp. 582–588, 2002.
[27] X. Wu, "Review of alloy and process development of TiAl alloys," 2006.
[28] F. Appel, J. D. H. Paul, and M. Oehring, *Gamma titanium aluminide alloys : science and technology*. Wiley-VCH, 2011.

## Appendix I

Notation

**Avg** - Average
**Cond** – Conduction
**CFD** – Computational Fluid Dynamic
**FEM** – Finite Element Method
**Rad** – Radiation
**RMSE**- Root Mean Square Error
**Obox** - Oil mean temperature between fluid nodes
***a*** - Constant for convective correlations
***A*** - Contact area between nodes [$m^2$]
**b** - Constant for convective correlations
***c*** - Constant for convective correlations
**c** - Specific heat capacity [J/K]
***C*** - Compressor housing node
**d** - Constant for convective correlations
***D*** - Diameter [m]
***e*** - Mechanical losses model parameter
***F*** - Form factor [-]
**FL** – Full Load
***h*** - Convective heat transfer coefficient [$W/(m^2K)$]
**H1** - Turbine backplate node
**H2** - Central housing node

**H3** - Compressor backplate node
**H4** - Internal metal node close to the turbine backplate
**H5** - Internal metal node at the centre of the central housing
**H6** - Internal metal node close to the compressor backplate
**H7** - Bearing node close to the turbine backplate
**H8** - Bearing node at the centre of the central housing
**H9** - Bearing node close to the compressor backplate
**IT** - Turbine inlet
***K*** - Conductance term, conductance matrix
***L*** - Distance between nodes [m]
***M*** - Conductance terms submatrix
***N*** - Rotational speed [r/min]
**Nu** - Nusselt number
**O1** - Oil node, before the shaft
**O2** - Oil node, after losses
**O3** - Oil node, before the last heat flux term
**OD** - Compressor diffuser outlet
**OI** - Oil inlet
**OO** - Oil outlet
**OT** - Turbine outlet
**Pr** - Prandlt number [-]
$\dot{\mathbf{q}}$ – Heat flux
$\dot{\mathbf{q}}$**'**- Virtual source term of heat flux
**R** - Radius of the external surface of central housing measured from the shaft
***r*** - Radius [m]
***Re*** - Reynolds number [-]
**S1** - Shaft node, turbine side
**S2** - Shaft node, central
**S3** - Shaft node, compressor side
***T*** - Time [s]
***T*** - Temperature [K]
**T** - Turbine node
**W** - Water node
$\dot{\mathbf{W}}$ Isentropic power
***Y*** - Heat flux fraction [-]
$\Lambda_{\mathbf{axial}}$ - Axial thrust in the bearings [N]
$\boldsymbol{\lambda}$ - Thermal conductivity [W / (m K)]
***m*** - Mass flow rate [kg / s]
$\Delta \boldsymbol{T}$ - Temperature difference [K]
***B*** - Central housing length distribution
$\boldsymbol{\gamma}$ - Central housing length distribution
**μ** - Dynamic viscosity [kg/(s·m)]

## Subscripts

**B** - Oil film mean line
**BH** - Bearing Housing
**C(OP)** - Coefficient as function of the engine operating point
**Bc** - Temperature boundary condition
**e** - External radius
**FL** – Friction Losses
**H** - Intermediate metal nodes layer
**I** - Internal radius
**ij** - Interaction between two adjacent nodes
**M** - Bearings bush
**X** - Unknown temperature
**p** - At constant pressure
**s** – Shaft